Quality assessment of laser cladded HSS coatings with deep penetration into base material to obtain a smooth gradient of properties in coating-substrate interface

S. Ločs[1,2] and I. Boiko[1,*]

[1]Riga Technical University, Faculty of Mechanical Engineering, Transport and Aeronautics, Institute of Mechanical Engineering, Viskalu street 36A, LV-1006 Riga, Latvia
[2]Daugavpils University, Faculty of Natural Sciences and Mathematics, Parades street 1, LV-5401 Daugavpils, Latvia
[*]Correspondence: irina.boiko@rtu.lv

Abstract. The present research is dedicated to the study of influence of coaxial laser cladding (CLC) process parameters onto values of alloying components content in the coatings, morphology as well as the influence of post-cladding heat treatment on the quality and mechanical properties of coatings. The research is based on a hypothesis that applying of first layer of coatings onto steel substrate with keyhole in penetration allows achieving smooth gradient of properties of the coating-substrate system. As a result it may provide a smooth distribution of the internal residual stresses in interface as well as the better resistance to external stress during cyclic load in tool operation processes: metal forming, stamping etc. Experimental work was carried out using CLC system, which consists of industrial robot Kuka and 1 kW IPG Yb-fiber laser, integrated to the coaxial powder supplying cladding head. The regularities of formation of High Speed Steel AISI M2 cladding coatings created by different regimes were studied by deposition onto EN 41Cr4 and C80U steel substrates. The quality of achieved coatings has been evaluated by examination of morphology of transverse cross-sections, coatings geometrical features, elemental composition and microhardness distribution inside coatings. Additionally detailed assessment of coating thickness and content of alloying elements using statistical methods has been performed. As a result of the research done the degree of influence of chosen CLC process parameters onto quality characteristics were estimated. The most appropriate cladding regime for used method was proposed.

Key words: coaxial laser cladding, HSS coating, keyhole in penetration, quality.

INTRODUCTION

Shortage of material and energy resources aids development and application of progressive technologies, which help to ensure the maximal performance indicators of machines in balance with economic efficiency and the minimal harm to environment. At the same time, the introduction of the thermal coating technologies makes it possible to improve the ecological compatibility of production by replacing hazardous galvanic technologies (Ločs & Boiko, 2015).

Coaxial laser cladding (CLC) is a progressive method of applying coating, which is widely used for improvement of mechanical and exploitation properties of products. This method allows applying of functional and protective coatings with a strong metallurgical bound with base material by minimal thermal impact on the item (Schneider, 1998; Toyrserkani et al., 2005). Thanks to a range of advantages in comparison to thermal spraying and welding processes this method is widely used for hardfacing, refurbishment and even for building up (Additive Manufacturing) of expensive machine elements and tooling (turbine parts, engine components, metal forming tools etc.) (Tabernero et al., 2011; Weisheit et al., 2013).

Meanwhile, despite of process positive points, producing defect free coatings of tool steel materials is still problematic, because tool steels are hardly suitable for welding due to a high content of carbon and alloying elements. Frequent defects are pore and crack formations in clad layers (Pleterski et al., 2011; Kattire et al., 2015; Zeng et al., 2016).

The pores can appear primarily due to insufficient shielding of melted zone, due to the moisture from the powder, due to evaporation process in the molten pool during laser irradiation of metallic surface.

In its turn the phenomenon of cracking is associated with the fact that melting by high energy of laser beam causes high heating and cooling rate which create a rigid temperature regime in the near surface layers. Thus, a sharp thermal gradient combined with a high rate of solidification in the melting region causes formation of metastable phases and as a consequence cracking of coatings (Benyounis et al., 2009; Candel et al., 2013; Telasang et al., 2014; Cao et al., 2016). As a result, mechanical properties and fatigue strength of the components significantly decrease, which can lead to premature failure and breakdown of the product. That's why the laser cladding technology may have one of the limiting factors to introduction into the surfacing processes (Grigoryants et al., 2006; Luo et al., 2016).

Therefore, in order to obtain qualitative coatings with high mechanical properties and fatigue life, the enhancement of laser cladding technology is still an actual issue.

The aim of this research is to determine the degree of influence of CLC process parameters onto values of alloying components content in the coatings, morphology as well as the influence of post-cladding heat treatment on the quality and mechanical properties of coatings. The research is based on a hypothesis that applying of first layer of coatings onto steel substrate with keyhole in penetration ensures smooth gradient of properties both for the similar and for dissimilar material combinations in coating-substrate interface. As a result such a technique may provide a smooth distribution of the internal residual stresses as well as better resistance to external stress during cyclic load in tool operation processes: metal forming, stamping etc.

MATERIALS AND METHODS

High-speed steels (HSS) demonstrate high strength, hardness and wear resistance by application of appropriate heat treatment. Along with the application for cutting tools, these steels can also be used for producing of die tools. Thus, they are operated under especially severe conditions, at pressures in above of 2,000 MPa and heating to temperatures of 300–500 °C for mass and large-scale production, when it is necessary to ensure high durability of the die tooling (Adaskin, 2017).

The filler material used in this research was Tungsten-Molybdenum HSS powder AISI M2 of spherical shape with particle size 53−150 µm. For substrates high carbon steels EN 41Cr4 and C80U plates were used with dimensions of 100 x 100 x 10 mm. In total four plates (by two of each material) were processed. The work surfaces of plates were mechanically grinded before treatment. Chemical compositions of the materials are listed in the next (Table 1).

Table 1. Chemical composition of powder AISI M2 (1), substrate EN 41Cr4 (2) and C80U (3)

	Element content, wt% (Fe in balance)						
	C	Mn	Si	Mo	Cr	V	W
1	0.85−1.05	0.20−0.40	0.20−0.40	4.50−5.50	3.75−4.50	1.60−2.20	5.50−6.80
2	0.36−0.44	0.50−0.80	0.17−0.37	−	0.80−1.10	−	−
3	0.75−0.85	0.10−0.40	0.10−0.30	−	−	−	−

Experimental work was carried out using CLC system, which consists of industrial robot KR30HA (Kuka) with the integrated coaxial powder supplying cladding head WT03 (Permanova Lasersystem) and Yb-fiber laser YLR 1000 (IPG Laser) with 100 µm optical fiber and 1,000 W power supply. Optical system provides laser beam spot size in a focus plane of about 570 µm with a Gaussian intensity distribution. Powder mass feeding performed with the powder feeder TWIN-10-C (Sulzer Metco), where the argon was used as a carrier gas and as a shielding gas to prevent oxidation of the powder and a molten pool. The laser cladding equipment is presented in the next (Fig. 1).
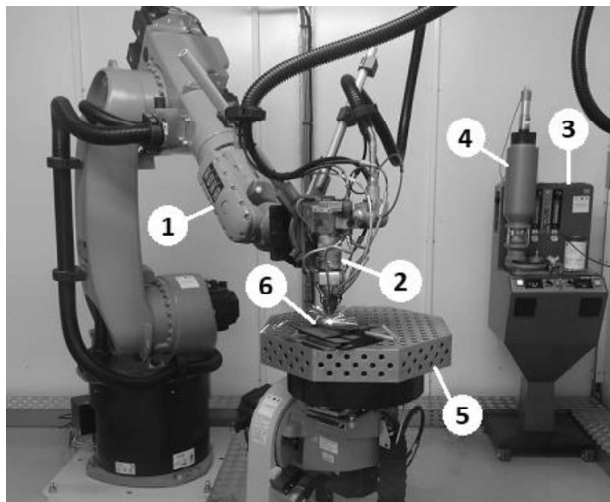

Figure 1. Laser cladding equipment: 1 − industrial robot KUKA; 2 − cladding tool; 3 − powder feeder; 4 − powder insert; 5 − table of positioner; 6 − workpiece.

Coatings during laser cladding were created by sequential overlapping of single cladding tracks. The cladding head all along process was located perpendicular to the surface being treated, directing laser beam toward the surface of the sample with stand-off distance 8 mm from the nozzle end. In order to establish interaction of three parameters with two values onto coating quality and properties the experimental research was carried out using experimental design (DOE) in form of two level full factorial

design 2^3 (Table 2). Thereafter 8 track coatings (approx. 8 mm wide) were deposited on each plate on the top surface of samples. For each coating 2 cross-sections were studied: produced coatings with prepared cut-off samples are displayed in the next (Fig. 2).

Table 2. Studied process factors and levels of variation

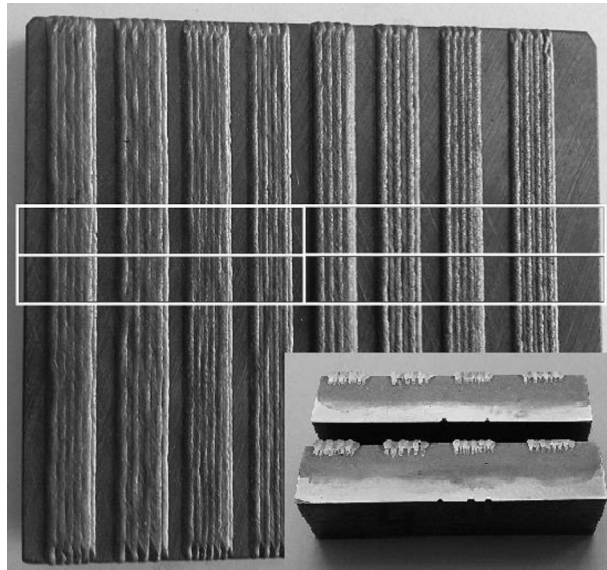| Factors	Designation	Levels		
		Upper (+1)	Nominal (0)	Lower (-1)
Overlap ratio, %	OR	50	40	30
Cladding speed, mm min^{-1}	V_C	1,500	1,200	900
Powder feed rate, g min^{-1}	F_P	10	7.5	5

Figure 2. Laser cladded plate with cut-out scheme and produced specimens of experimental coatings cross-sections.

The experiment plan includes a combination of parameters such as the overlap ratio between adjacent cladding beads (50% and 30%), the cladding speed (900 mm min^{-1} and 1,500 mm min^{-1}) and the powder mass feed rate (5 g min^{-1} and 10 g min^{-1}). Disposition of the laser beam focal plane was 1 mm above the treatable surface (defocused beam), which was taken on the basis of the previous study of single bead formation (Ločs et al., 2017). The focus plane of the powder flow was coincided with laser beam focus. The following process parameters were fixed to operate: laser power 1,000 W; carrier gas flow (Ar) 5 L min^{-1}; shielding gas flow (Ar) 16 L min^{-1}. The samples were preheated to a temperature of 250 °C prior to treatment and the temperature regime was the same for each subsequent coating.

With aim to establish the influence of process parameters (overlap ratio, scanning speed and powder mass feed rate) on the coating characteristics predictive equations were created using regression analysis. For evaluating of statistical significance created models were tested by analysis of variance method (ANOVA). The relationship between CLC parameters and output responses were analysed and described in details. Therewith

the impact of appliance of post-cladding heat treatment was also obtained. By this reason one group of samples with produced coatings had post-cladding tempering (by plate heating in a furnace at 600 °C for 2 h and then cooling in air) (PCT), but the second group remained untempered. Plates with experimental coatings were transversely cross-sectioned, then polished and etched with Nital (4%). Examination of coatings transverse cross-sections was conducted by means of morphological observation using scanning electron microscope TESCAN-VEGA-LMU II (SEM). Elemental composition of the main alloying components in the microstructure was determined by energy dispersive spectrometry EDS analysis (EDS module INCAx-act Oxford Instruments). Microhardness profiles were measured along the transversal cross-section from the top of the coating to the substrate base using the Vickers hardness tester (Innovatest Nexus 4000). Measurements were performed under 200 g load and 10 s hold time on the each measurement point.

RESULTS AND DISCUSSION

The efficiency of a hardfaced coating primarily depends on its microstructure, which is defined by the chemical composition and solidification rate of coatings. Accordingly, the effect of processing parameters and their interactions should be controlled to optimize the properties.

During SEM analysis produced coatings were evaluated by measures of coatings thickness (H) and content of strong carbide-forming elements such as V, Cr, Mo, W in surface layer, which for analysis decided to express in the form of total amount of alloying elements mass fractions (A). According to this coating thickness deposited on 41Cr4 steel substrate designated as (H_1) and coating thickness for C80U (H_2) respectively. Similarly to this, sum of alloying elements in coating deposited on 41Cr4 steel substrate labelled as (A_1) and content of alloying elements in coating on C80U steel (A_2). The used matrix of DOE with mean results of measures (experimental responses) is presented in the Table 3.

Table 3. Experimental design matrix, thickness and sum of alloying elements V, Cr, Mo, V

Regime No.	OR, %	V_C, mm min^{-1}	F_P, g·min^{-1}	$\overline{H_1}$, μm	$\overline{H_2}$, μm	$\overline{A_1}$, wt%	$\overline{A_2}$, wt%
1	50	900	5	581	516	6.48	4.81
2	30	900	5	376	391	5.31	4.58
3	50	1,500	5	325	331	5.44	3.87
4	30	1,500	5	215	209	5.03	3.91
5	50	900	10	721	729	8.28	8.56
6	30	900	10	492	485	7.95	8.35
7	50	1,500	10	500	489	8.07	7.00
8	30	1,500	10	243	320	7.22	7.50

Morphology

In order to test the hypothesis of the current research, the coatings were created with significant penetration into substrate, which have keyhole geometry due to a high power density. As a result, depth of penetration was in range 1.8 to 2.4 mm (Fig. 3, a), which was determined as a sum of lengths ($D = D_1 + D_2$) of interfusion zone (IZ) and keyhole in penetration (KP).
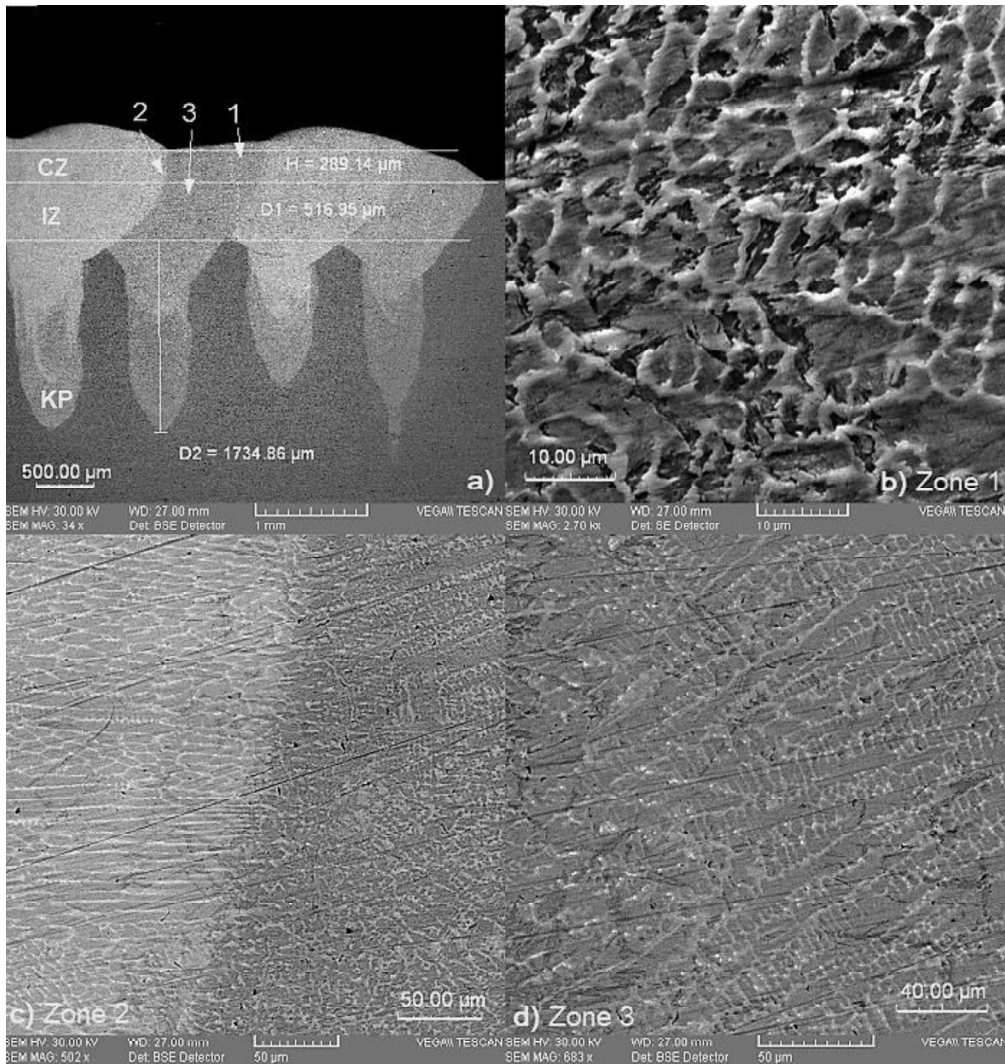
Figure 3. SEM images of cross-section of the laser cladding coating (a) deposited on 41Cr4 substrate according to regime No.2 with shown geometrical measures (CZ – clad zone; IZ – interfusion zone; KP – keyhole in penetration) and higher magnification electron images of denoted regions: 1 – zone near the surface (b); 2 – region between single tracks (c); 3 – the center zone of single track (d).

Detailed consideration of the SEM micrographs of the samples cross-sections was conducted to examine the morphology, geometrical parameters and defects of fabricated laser cladding (LC) coatings. The microstructure of M2 coatings on 41Cr4 and C80U substrates near the surface region was mostly equiaxed (Fig. 3, b), which could be attributed to a uniform heat flow in all the directions (Majumdar et al., 2005). The size of intercellular spacing ranged between 2–5 μm. However in the clad zone (CZ) and in IZ, i.e. in the middle part of a single clad bead and areas near the substrate had directionally solidified cellular-dendritic microstructure, growing almost perpendicularly from the fusion line (i.e. crystallization front between single tracks or with the base material) to the center zone of clad bead (Fig. 3, c, d). The micrograph of

zone with columnar dendrites structure is presented in the next (Fig. 3, d): dark regions attributed to dendritic regions, while interdendritic regions are white. As it's noted by (Navas et al., 2005; Candel et al., 2013) M2 LC coatings have fine cellular-dendritic structure consisted of martensite and carbide eutectic at grain boundaries of different kinds of M_nC_m (where M represents Cr, Mo, W, V). The improvement of the microstructure in HSS steels through solidification depends on the cooling rate and chemical composition of the alloy (Boccalini & Goldenstein, 2001; Benyounis et al., 2009).

The size of intercellular and primary dendritic spacing obtained in this study varied between 4–10 µm and secondary dendritic arm spacing in range between 2–4 µm respectively. Grains become finer by increasing cladding speed and by increasing distance between contiguous cladding tracks, which is referred to increasing cooling rate, due to reduction of heat input of the acting laser beam as well as influence of conducted heat of adjacently deposited cladding bead.

When comparing the quality of all produced coatings on both substrates it was found that most of the cracks contain coatings on C80U steel substrate. Furthermore appliance of post-cladding heat treatment insignificantly reduced this kind of defect. In this case by investigation of microstructure it was noticed that cracks had propagation along intergrain boundaries (Fig. 4, a, b), which could be characterized as solidification cracks also known as hot cracks. This may be an explanation of why the tempering didn't affect the decrease of crack formation.
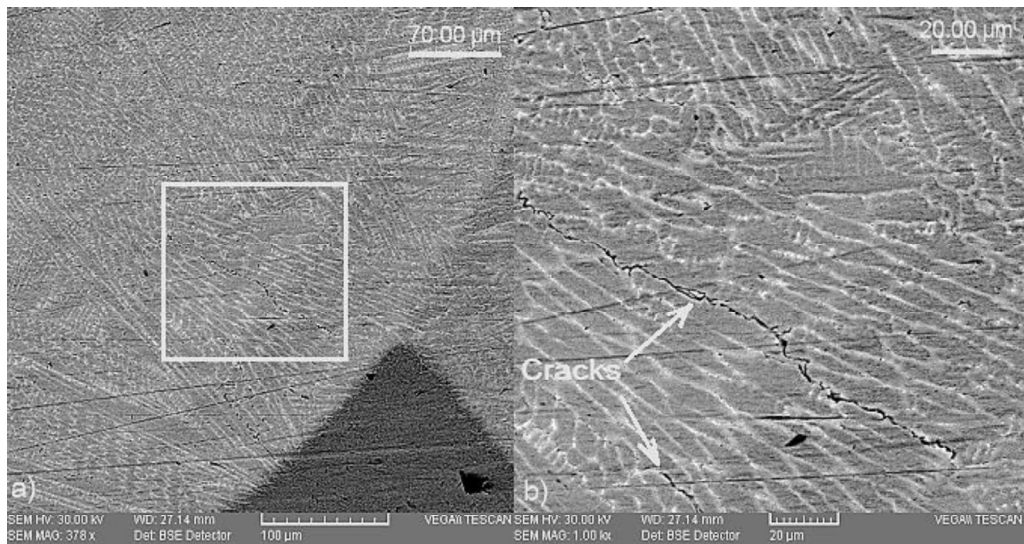

Figure 4. SEM images of the coating in interfusion zone (a) and higher magnification image of selected area (b) with microcracks at the grains boundaries.

It has to be pointed that the most of the cracks corresponded to 50% of clad tracks overlap, which contributes to the formation of a thicker coating. In this case, cracks can be formed due to a secondary remelting of previously deposited cladding track, which can cause formation of different interval of fragility during melt solidification. Concerning coatings produced on the base steel 41Cr4 there were also some cracks

detected, mainly on the thickest coatings produced. Consequently, to lower the formation of cracks, it is necessary to determine the optimal coating thickness.

The presence of pores of 100–300 μm was also found, mostly in the keyhole penetration. This phenomenon was described earlier in (Ločs et al., 2017), which related to the high power density of the acting laser beam, due to rapid evaporation of the molten material and producing air bubbles. Nevertheless the smallest content of pores pertained to coatings created at the higher cladding speed, which agrees well with (Katayama, 2010) study, where one of the confirmed action to prevent of the pore formation in the keyhole referred to increasing of the process speed.

Data analysis

In this study the influence of experimental factors was estimated by determining of mathematical models based on the measured parameters (thickness and sum of alloying elements in coatings) according to the design matrix. In order to confirm mathematical model coefficient of determination (R^2) was also calculated. Additionally ANOVA was completed for estimating of statistical significance of developed models by applying confidence level of 95% (*P*-value of 0.05).

Coating thickness

The range of thicknesses of produced coatings varied from 185 to 760 μm , the largest value as it has been expected corresponded to the largest amount of powder, the lowest scanning speed and for the highest value of overlap ratio (OR 50%). Fig. 5 depicts coatings thickness distribution relative to combination set of parameters.

As it can be seen this parameter shows practically identical distribution for both substrates. The decrease in thickness is accompanied by an increase in cladding speed and distance between adjacent cladding beads.
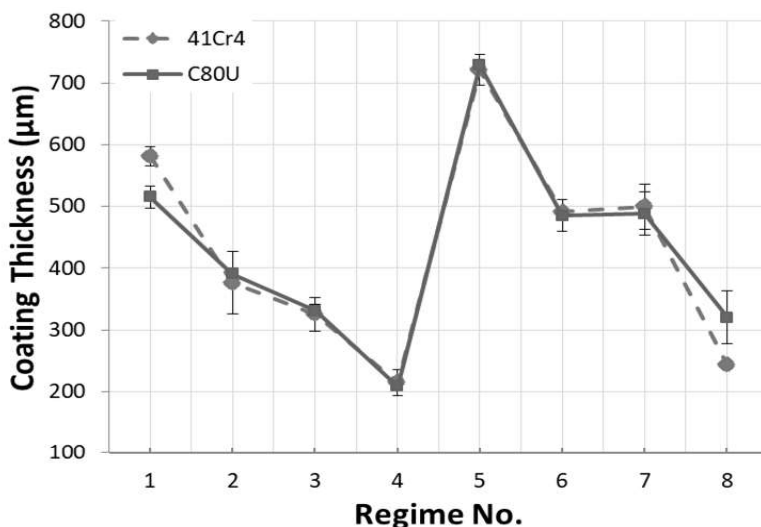

Figure 5. Variation of coatings thikness in relation to regimes.

Table 4 represents ANOVA for the coatings thickness. F-values of 42.41 for coatings produced on 41Cr4 steel substrate and of 45.52 for coatings on C80U steel substrate indicate the models are significant. P-values greatly less than 0.05 indicate that overlap ratio (OR), scanning speed (VC) and powder mass feed rate (FP) are all significant model terms. Especially the scanning speed turned out to be a dominant factor. Coefficients of determination (R^2) are very high and equal to 0.95 for both of H_1 and H_2 parameters and prove a high correlation between the experimental and the calculated results.

Table 4. ANOVA for the coatings height: DF – degree of freedom, SS – sum of squares, MS – mean squares

For 41Cr4 steel substrate					
Source	DF	SS	MS	F	P
Model	3	205,019	68,340	42.41	0.002
OR	1	80,400	80,400	49.89	0.002
V_C	1	98,513	98,513	61.13	0.001
F_P	1	26,106	26,106	16.20	0.016
Residual	4	6,446	1,612		
Total	7	211,465			
For C80U steel substrate					
Source	DF	SS	MS	F	P
Model	3	170,302	56,767	45.52	0.002
OR	1	54,182	54,182	43.45	0.003
V_C	1	74,522	74,522	59.76	0.002
F_P	1	41,598	41,598	33.36	0.004
Residual	4	4,988	1,247		
Total	7	175,290			

The mathematical models for coating thickness (H) and process parameters in terms of actual factors are given in the following expressions:

$$H_1 = 303.1 + 10.03\ OR - 0.367\ V_C + 22.85\ F_P, \qquad (1)$$

$$H_2 = 274.1 + 8.23\ OR - 0.322\ V_C + 28.84\ F_P. \qquad (2)$$

These equations (1 and 2) mirror of showed in Fig. 5 and demonstrate that powder feed rate has a positive effect onto coating thickness. The same effect presents OR parameter, namely by increasing percentage of overlap coating thickness enlarges. However, coating thickness decreases by increasing of cladding speed.

Elemental composition

In order to investigate relations between process parameters and content of the carbide-forming elements in clad zone (CZ) of coatings such as Cr, Mo, W, V elemental composition was measured on selected areas (Fig. 6, a) of all cross-sectioned coatings using EDS analysis (Fig. 6, b). The results of the generalized data for each regime are presented earlier in the (Table 3).
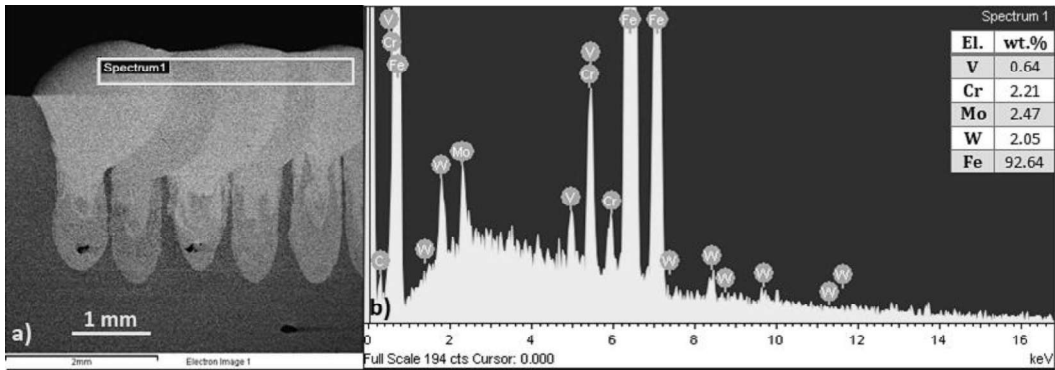
Figure 6. Cross-section SEM image of coating deposited by 1st regime (a) and spectra of X-ray emission for alloys present (b).

On the whole it was noticed that significant decrease of alloys after laser cladding is typical for all coatings achieved, which can be explained with the fact that by operating at a high power density quite huge intermixing occurs between melt and base and it causes ferrugination of cladded coatings. Iron consecration in upper layer of coatings correlates with observed parameter A_i (in form of the total amount of Cr, Mo, W, V), which was further used as the model's output response to determine the relationship with processing parameters. As it is shown below (Fig. 7), powder adding significantly increase content of alloys in the coatings. Maximal value corresponds to the 5th regime of DOE. Overall the plot of components distribution appeared very similar to previously presented by graph for coatings thickness. The coefficients of correlation (R) between two estimated parameters H_1 and A_1 as well as between H_2 and A_2 are equal to 0.65.
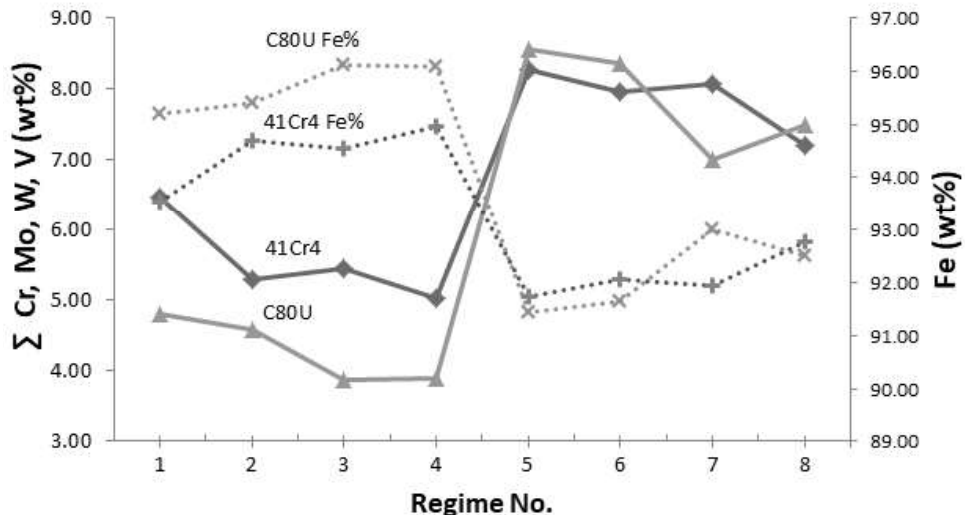

Figure 7. Variations of alloying elements content in coatings in relation to regimes.

1104

Table 5 shows ANOVA for the total amount of alloy components. The models F-values of 65.17 for coatings on 41Cr4 steel substrate and 144.99 for coatings on C80U steel substrate represent high statistical significance. In this case powder feed rate (F_P) and cladding speed (V_C) are significant model terms. Therewith main effect showed powder feed rate. However overlap ratio (OR) showed significance only for processing on 41Cr4 steel substrate, but for C80U steel it didn't.

Table 5. ANOVA for the total amount of Cr, Mo, W, V: DF – degree of freedom, SS – sum of squares, MS – mean squares

For 41Cr4 steel substrate					
Source	DF	SS	MS	F	P
Model	3	12.304	4.101	65.17	0.001
OR	1	0.952	0.952	15.13	0.018
V_C	1	0.633	0.633	10.06	0.034
F_P	1	10.719	10.719	170.31	0.000
Residual	4	0.252	0.063		
Total	7	12.56			
For C80U steel substrate					
Source	DF	SS	MS	F	P
Model	3	27.356	9.119	144.99	0.000
OR	1	0.001	0.001	0.02	0.889
V_C	1	2.025	2.025	32.20	0.005
F_P	1	25.330	25.330	402.75	0.000
Residual	4	0.252	0.063		
Total	7	27.608			

The below given empirical relationships represent that the content of alloying elements increases by decreasing of cladding speed and by increasing of powder feed rate.

$$A_1 = 2.992 + 0.0345\ OR - 0.0009\ V_C + 0.4630\ F_P, \qquad (3)$$

$$A_2 = 2.796 - 0.0013\ OR - 0.0017\ V_C + 0.7118\ F_P. \qquad (4)$$

For these models R^2 has also very high indexes: values of 0.97 and 0.98 for coatings produced on 41Cr4 steel substrates and for coatings produced on C80U steel substrates respectevely. That denotes that the developed mathematical models are in a good agreement with the experimental data.

Mechanical properties

Fig. 8 demonstrates distribution profiles of Vickers microhardness along depth of transversal cross-sections in coating-substrate system. These profiles refer to the coatings created by the first four regimes of the DOE on both steel substrates (C80U and 41Cr4). The first approach includes the difference in overlap ratio (OR) of single cladding tracks and the difference in cladding speed (V_C) (solid lines); the second one corresponds to the similar area of regimes with applicable post-cladding tempering (+PCT) in addition (dash lines).

As it is seen the distribution of hardness values had consequent gradual decrease in depth. The hardness of clad zones of coatings varied in range of 830–500 HV0.2, depending on the combination of process parameters. Generally M2 coatings had 2–3 times highest values of hardness compared with substrates (~240–290 HV0.2, where the lowest value corresponds to 41Cr4 steel). Basically the highest hardness of clad zones corresponded to the coatings produced with OR50% and the lowest cladding speed concerning to both steel substrates (Fig. 8, a, b, c – profile 1). This outcome is well consistent with the previously obtained content of carbide-forming elements.
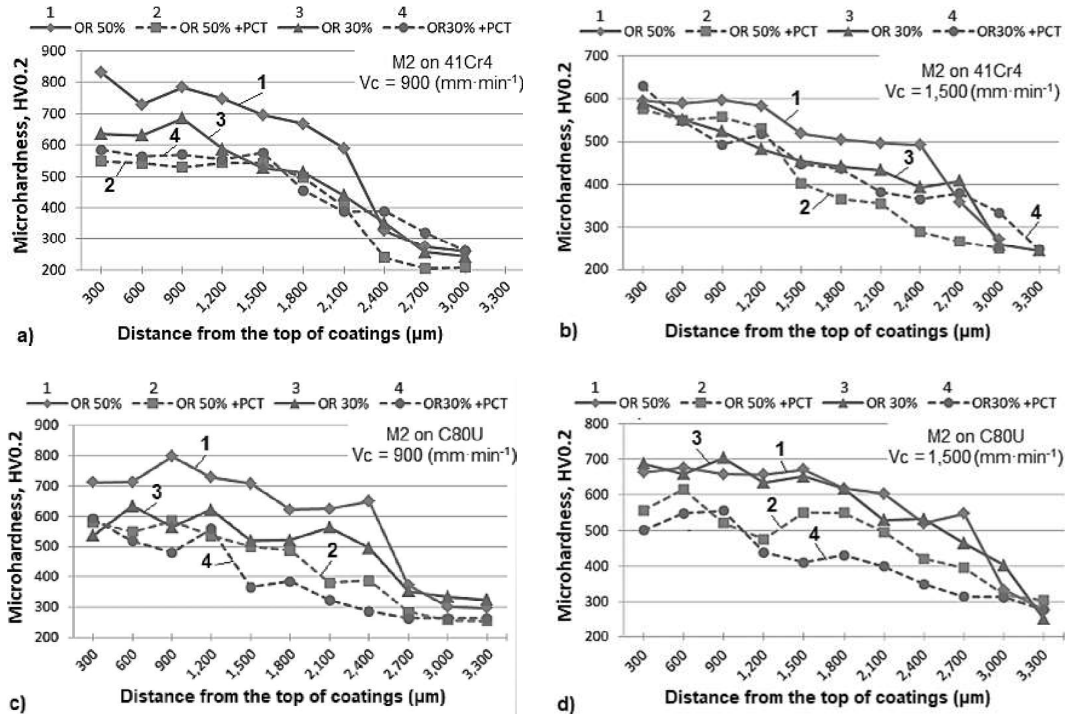

Figure 8. Vickers microhardness profiles on transverse cross-sections of coatings as function of depth: (a) M2 coatings deposited on 41Cr4 substrate: $V_C = 900$ mm min^{-1}; (b) M2 coatings deposited on 41Cr4 substrate: $V_C = 1,500$ mm min^{-1}; (c) M2 coating deposited on C80U substrate: $V_C = 900$mm min^{-1}; (d) M2 coating deposited on C80U substrate: $V_C = 1,500$ mm min^{-1}.

As can be seen tempering mostly leads to a considerable decrease of hardness (profiles 2 and 4). However, on the other hand the profiles of post-clad tempering show more gradual variation of hardness towards the base material. Therewith, it was noticed, that hardness profiles of coatings produced with the lesser ratio of overlap (OR30% – profiles 3) demonstrate very close values to the PCT profiles, only excepting the case of C80U substrate and the highest cladding speed (Fig. 8, d – profiles 3). However this profile demonstrates a smoother transition of hardness towards the base, in comparison to profile 1, which in all cases showed abrupt transitions. That's why change of properties of this type could be the reason for fewer cracks in the coatings produced with 30% overlap.

Since the hardness index implicitly correlates to the strength of the material, this fact may be juxtaposed with the conditions for the distribution of residual stresses in the coating-substrate system. Based on the analysis of the hardness distribution, it may be assumed that coatings with keyhole in penetration affect the gradient of properties in depth. Thus, by controlling the size and shape of the penetration, by means of regulating the process parameters, it is possible to achieve a smooth redistribution of internal residual stresses, by reducing the stress in coating-substrate interface. Thereby applying such a technology may exclude the deposition of the buffer layer for hardfacing and cladding in surfacing applications. This method can also improve the fatigue strength of the coatings.

CONCLUSIONS

In current study laser cladding coatings were deposited using AISI M2 powder on EN 41Cr4 and C80U steel substrates. It was studied the influence of process parameters including overlap ratio between adjacent cladding beads, cladding speed and powder mass feed rate onto content of alloying elements and thickness of coatings and the influence of post-cladding tempering on the coatings quality. The quality of coatings has been evaluated by examination of morphology of transverse cross-sections, coatings geometrical features, elemental composition, mechanical properties (microhardness); additionally detailed assessment of coating thickness and content of alloying elements using statistical methods has been performed.

As a result the followings conclusions may be drawn:
- Coatings were created with significant penetration into substrate (1.8 to 2.4 mm), which have keyhole geometry due to a high power density;
- The microstructure of coatings was mostly equiaxed near the surface region (with grain size of 2–5 μm); in the middle part of a single clad bead and areas near the substrate region were cellular-dendritic structures (intercellular and primary dendritic spacing 4—10 μm, secondary dendritic arm spacing 2–4 μm);
- Grains become finer by increasing cladding speed and by increasing distance between contiguous cladding tracks;
- The presence of solidification cracks and gas pores was found. Cracks were mostly observed in coatings on C80U steel substrate and appliance of post-cladding heat treatment insignificantly reduced them. Reduction of overlap ratio and rise of cladding speed may lower the formation of cracks. Pores were most often located in keyhole penetration. Elimination of the pore formation is most likely to be achieved by increasing of cladding speed.
- Thickness of produced coatings varied from 185 to 760 μm. The largest value corresponded to the 5th regime of experimental design (OR 50%, $V_C = 900$ mm min^{-1}; $F_P = 10$ g min^{-1}). Maximal concentration of alloying carbide-forming elements (Cr, Mo, W, V) in the coating also corresponded to the 5th regime.
- ANOVA test of developed mathematical models for coating thickness indicated significant relationships between the process parameters and coating thickness. Results of the analysis demonstrated that scanning speed was a dominant factor, i.e. by increase of cladding speed coating thickness decreased. However both overlap ratio and powder feed rate had positive effect.

- Statistical analysis of alloying elements content showed adequacy of designed models, which represented that the content of them increases by decreasing of cladding speed and by increasing of powder feed rate. However overlap ratio showed significance only for processing on 41Cr4 steel substrate, but for C80U steel it didn't.
- Developed mathematical models can be used to predict coating thickness and content of alloying element in it within a confidence level more than 95%. According to this the optimal regime can be determined by relying onto created models.
- The analysis of microharndess distribution revealed that by producing coatings with 30% of overlap (i.e. larger distance between adjacent cladding beads) the smoother hardness profile was achieved. It was shown that coatings with keyhole in penetration may affect the gradient of properties in depth. Eventually it is assumed that by controlling size and shape of penetration, it is possible to achieve a smooth redistribution of internal residual stresses, by reducing the stress gradient in coating-substrate interface. Applying of this technology may exclude the deposition of the buffer layer for hardfacing and cladding in surfacing applications.
- As a result, in order to minimize the gradient of residual stresses in the coating it is preferable to perform laser cladding of the first layer of coating according to 8th regime (OR 30%, $V_C = 1,500$ mm min^{-1}; $F_P = 10$ g min^{-1}).

REFERENCES

Adaskin, A.M. 2017. *Tool materials in Mechanical Engineering*. Moscow, Infra-M, 319 pp. (in Russian).

Benyounis, K.Y., Fakron, O.M. & Abboud, J.H. 2009. Rapid solidification of M2 high-speed steel by laser melting. *Materials and Design* **30**, 674–678.

Boccalini, M. & Goldenstein, H. 2001. Solidification of high speed steels. *International Materials Reviews* **46**(2), 92–115.

Candel, J.J., Franconetti, P. & Amigó, V. 2013. Study of the solidification of M2 high speed steel Laser Cladding coatings. *Revista de Metalurgia* **49**(5), 369–377.

Cao, H.T., Dong, X.P., Pan, Z., Wu, X.W., Huang, Q.W. & Pei, Y.T. 2016. Surface alloying of high-vanadium high-speed steel on ductile iron using plasma transferred arc technique: Microstructure and wear properties. *Materials & Design* **100**, 223–234.

Grigoryants, A.G., Shiganov, I.N. & Misyurov, A.I. 2006. *Technological processes of laser processing*. Moscow, Bauman Moscow State Technical University, 664 pp. (in Russian).

Katayama, S. 2010. Understanding and improving process control in pulsed and continuous wave laser welding. In: *Advances in laser materials processing*. Woodhead Publishing Limited, Cambridge, pp. 181–210.

Kattire, P., Paul, S., Singh, R., Yan, W. 2015. Experimental characterization of laser cladding of CPM 9V on H13 tool steel for die repair applications. *Journal of Manufacturing Processes* **20**, 492–499.

Ločs, S. & Boiko, I. 2015. Investigation of Plasma Spray Deposition of Cermet Coatings. In*: 9th International Simposium on Powder Metallurgy, Surface Engineering, New Composite Materials, Welding.* Minsk, Belarus, pp. 122–125. (in Russian).

Ločs, S., Boiko, I., Drozdovs, P., Dovoreckis, J. & Devoyno, O. 2017. Investigation of coaxial laser cladding process parameters influence onto single pass clad geometry of tool steel. *Agronomy Research* **15**(4), 1659–1673.

Luo, K.Y., Jing, X., Sheng, J., Sun, G.F., Yan, Z. & Lu, J.Z. 2016. Characterization and analyses on micro-hardness, residual stress and microstructure in laser cladding coating of 316L stainless steel subjected to massive LSP treatment. *Journal of Alloys and Compounds* **673**, 158–169.

Majumdar, J.D., Pinkerton, A., Liu, Z., Manna, I. & Li, L. 2005. Microstructure characterisation and process optimization of laser assisted rapid fabrication of 316L stainless steel. *Applied Surface Science* **247**(1–4), 320–327.

Navas, C., Conde, A., Fernández, B.J., Zubiri, F. & de Damborenea, J. 2005. Laser coatings to improve wear resistance of mould steel. *Surface and Coatings Technology* **194**(1), 136–142.

Pleterski, M., Tusek, J., Muhic, T., Kosec, L. 2011. Laser cladding of cold-work tool steel by pulse shaping. *Journal of Materials Science and Technology* **27**(8), 707–713.

Schneider, M.F. 1998. *Laser cladding wth powder*. Twente (Netherlands), University, Dissetation, Enschede, 177 pp.

Tabernero, I., Lamikiz, A., Martínez, S., Ukar, E. & Figueras, J. 2011. Evaluation of the mechanical properties of Inconel 718 components built by laser cladding. *International Journal of Machine Tools and Manufacture* **51**(6), 465–470.

Telasang, G., Majumdar, J.D., Padmanabham, G., Tak, M. & Manna I. 2014. Effect of laser parameters on microstructure and hardness of laser clad and tempered AISI H13 tool steel. *Surface and Coatings Technology* **258**, 1108–1118.

Toyserkani, E., Khajepour, A. & Corbin, S. 2005. *Laser Cladding*. CRC Press LLC, New York, 263 pp.

Weisheit, A., Gasser, A., Backes, G., Jambor, T., Pirch, N. & Wissenbach, K. 2013. Direct Laser Cladding, Current Status and Future Scope of Application. In: *Laser-Assisted Fabrication of Materials*. In: Majumdar, J.D., Manna, I. (Eds.). Springer Heidelberg New York Dordrecht London, pp. 221–240.

Zeng, C., Tian, W., Liao, W.H., Hua, L. 2016. Microstructure and porosity evaluation in laser-cladding deposited Ni-based coatings. *Surface and Coatings Technology* **294**, 122–130.